Emergent Materials (2022) 5:1705–1716
https://doi.org/10.1007/s42247-022-00420-9

ORIGINAL ARTICLE

In vitro effects of the green synthesized silver and nickel oxide nanoparticles on the motility and egg hatching ability of *Marshallagia marshalli*

Yousef Mirzaei[1] · Samir M. Hamad[1] · Azeez A. Barzinjy[2,3] · Vinos M. Faris[1] · Masoud Karimpour[4] · Mukhtar H. Ahmed[5]

Received: 11 August 2022 / Accepted: 12 October 2022 / Published online: 21 October 2022
© Crown 2022

Abstract

Background Gastrointestinal nematodes are one of the serious health problems on the human society and in the livestock industry. *Marshallagia marshalli* is one of the most prevalent gastrointestinal nematodes in small ruminant, have subtle but more significant adverse effects on the health and fitness of their hosts.

Aim In this study, green synthesized nickel oxide (NiO) and silver (Ag) nanoparticles (NPs) have been checked to evaluate the possible antiparasitic effects of nickel oxide and silver nanoparticles on *Marshallagia marshalli.*

Methods The characterization of synthesized NiO NPs and Ag NPs was confirmed using the scanning electron microscopy (SEM), X-Ray diffraction (XRD), and UV–Visible spectroscopy. The adult worms were incubated with various concentrations of NiO and Ag NPs with the quantity of; 1, 2, 4, 8, 12, and 16 ppm for 24 h. Mobility and egg hatching abilities of the parasites were recorded at 4-h intervals.

Results The results showed that both of the nanoparticles NiO and Ag NPs have anthelmintic activity against *Marshallagia marshalli.* The anthelmintic effects increased with an increase in the concentration of nanoparticles and the incubation time.

Conclusion The outcome data concluded that Ag-NPs possess a higher level of efficacy than NiO NPs.

Keywords *Marshallagia marshalli* · Nickel oxide NPs · Silver NPs · Motility · Egg hatching

1 Introduction

Helminth infections are a serious threat to the human community and livestock industry [1]. Among parasitic worms, the nematodes have subtle but more significant deleterious effects on the health and fitness of their hosts [2]. These infections can lead to gastroenteritis and a decrease in animal health, productivity, and farm profitability [3]. *Marshallagia marshalli* is a prevalent nematode belongs to Trichostrongylidae family infecting the abomasum of domestic and wild ungulates and found in wide range of climatic zones from tropical ecosystems to temperate areas and even in Arctic (Irvine et al., 2000; Altaş et al., 2009; [4–8]. Multiple species and morphotypes of the genus *Marshallagia* are recognized nowadays [9],however, *M. marshalli* is the most important and can cause constipation, loss of appetite and weight, diarrhoea, and even death in severe cases in their hosts [10]. In wild ungulates, *M. marshalli* has negative consequences on fetus development and body condition [4, 11, 12]. Control measures to prevent economic losses of GIN nematodes in livestock are heavily dependent on the utilization of anthelmintic drugs; however, the repeated and often excessive use of these compounds over more than three decades has led to the development of anthelmintic resistance [13–15]. Moreover, the limited water solubility of some anthelmintic drugs have negative impact on their absorption

✉ Mukhtar H. Ahmed
ahmed-m@email.ulster.ac.uk

1 Scientific Research Centre, Soran University, Soran, Kurdistan Region, Iraq

2 Department of Physics, College of Education, Salahaddin University-Erbil, Erbil, Iraq

3 Department of Pshysics, Faculty of Education, Tishk International University, Erbil, Iraq

4 Department of Biology, Faculty of Sciences, Soran University, Soran, Kurdistan Region, Iraq

5 Sisaf Nanotechnology Drug Delivery, Ulster University, Belfast BT370QB, UK

and finally resultant clinical efficacy [16, 17]. In addition, the drug residues in animal products have deleterious effects on ecosystem and consumers [18, 19]. Therefore, there is an essential need to find new alternatives for control of GIN nematodes in the livestock industry.

A nanoparticle is a small particle that ranges between 1 and 100 nm in size. Untraceable by the human eye, nanoparticles can display suggestively diverse physical and chemical properties to their larger material counterparts. Due to their very small size, nanoparticles have a very large surface area to volume ratio when compared to bulk material, such as powders, plate and sheet. This feature enables nanoparticles to possess unexpected optical, physical and chemical properties, as they are small enough to confine their electrons and produce quantum effects. Some of the parasites established drug resistance, which increased the requirement for novel effective agents against parasitic infection or improvement of the present drugs and there is no vaccine available for the prevention of many parasitic infections. Nanobiotechnology have revealed extraordinary development in the treatment of parasitic infections. This is relying upon the exclusive properties of NPs including Ag NPs, Au NPs, NiO NPs, and other metallic oxide NPs that have shown excellent inhibitory effects against parasitic infections including insect larvae [20, 21]. New findings demonstrate that the nanoparticles could be considered as potential anti parasitic candidates [22]. The size of nanomaterials is ranged between 10 and 100 nm, therefore they present some outstanding properties, such as high surface area per volume and strong adhesion to surfaces. [23]. Currently, different types of nanoparticles with different structures including solid nanoparticles, polymeric nanoparticles, nanocrystals, and liposomes have shown broad development prospects in their applications as antimicrobial and antiparasitic drugs. These nanoparticles can be managed by oral, intra-gastric, duodenum, skin, pulmonary, intravenous, and other retreats based upon the demands of disease handling [24–27]. These nanoparticles have a small size and large surface area for effective interaction with bacteria, allowing nanoparticles to easily penetrate into bacteria and adhere to their cell membranes without degrading the nanoparticles (Taghavizadeh et al., 2022). If nanoparticles interact with the bacterial mitochondrial respiration chain, they can destroy or kill cells. These nanoparticles can penetrate the biological barriers, by enzymes, and direct the target, physical stability, effective intracellular distribution and accumulation, etc. [28, 29].

Nanotechnology is well-known as an established up-to-date technology with an unlimited range of applications that can be used in numerous physical, biological, biomedical, and pharmaceutical applications [30, 31]. Different nanoscale devices have been industrialized using several methods since nanotechnology was developed [32]. Recently, the eco-friendly green synthesis nanomaterial is being a vital approach for material scientists as a result of harmful issues related to physical and chemical techniques. Nowadays, a green synthetic approach particularly using different plant extracts is an upward trend in green chemistry that is an easy, cheap, and safe method for synthesizing nanoscale materials [20, 21, 33–36]. For instance, Baghbani et al. [37] showed that ZnO-NPs have considerable anthelminthic effects, depending on time and concentration. Moreover, the nanoparticle can induce severe oxidative/nitrative stress and DNA damage in *Teladorsagia circumcincta*. Adeel et al. [38] assessed the possible damaging impacts of NiO NPs on survival and reproduction of earthworms using the Organization for Economic Cooperation and Development (OECD) typical test procedure. They have likewise studied the effect of NiO NPs on biochemical biomarkers and oxidative DNA mutilation of earthworms.

The novelty of this study can be highlighted here, since the green synthesis method was used for synthesizing both nickel oxide (NiO) and silver (Ag) nanoparticles from the purified and fresh *Rhus coriaria* seed extraction. Then, the possible antiparasitic effects of these nanoparticles on *Marshallagia marshalli*, as one of the predominant gastrointestinal nematodes in small ruminants, have been investigated. The reason behind selecting Ag and NiO NPs refers to these NPs are widely used and they have anti-inflammatory, antiparasitic, and anti-bacterial properties with cytotoxicity behaviour against cancer cells. In addition, they have environmental applications in hazardous pollutants and dyes removal and serve like a capable agent in environmental cleanliness and safety.

2 Materials and methods

2.1 Chemicals and reagents

Nickel nitrate hexahydrate [Ni $(NO_3)_2{\cdot}6H_2O$], silver nitrate ($AgNO_3$), molecular weight 169.87 g/mol, purity > 99%, and sodium hydroxide pellets (NaOH) were purchased from Sigma-Aldrich Company. The other materials, solvents, and double-distilled water were obtained locally and utilized without extra purification. Double-beam UV–Vis spectrophotometer analysis (Super Aquarius spectrophotometer-1000) was used to confirm the formation of NiO and Ag NPs. X-ray diffraction (XRD) measurements were carried out using a PAN analytical X′Pert PRO (Cu Kα = 1.5406 A°), the scanning rate was 1°/ min in the $\theta^{-}2\theta$ range from 20 to 80°. Morphology and particle dispersion were investigated by field emission scanning electron microscopy (FE-SEM) (Quanta 4500). The chemical composition of the prepared nanostructures was analyzed by energy-dispersive X-ray spectroscopy (EDX) executed in the FE-SEM machine.

QAPCO QATAR PETROCHEMICAL COMPANY جامعة قطر QATAR UNIVERSITY

2.2 Preparation of the plant extraction

Fifty grams of the *Rhus coriaria* seed was added in to100 mL of double distilled water, and then, the mixture was boiled at 80 °C while stirred for 40 min. After that, the final solution was filtered by filter paper and the pure extract was kept in a fridge for additional usage.

2.3 Preparation of NiO and Ag nanoparticles

2.3.1 Preparation of NiO nanoparticles

In general, this study aimed to prepare NiO NPs using green synthesis method. *Rhus coriaria* extract utilized as a reducing, capping and stabilizing agents and nivklel nitrate utilized as a Ni ion source. In addition, Sodium hydroxide, NaOH, utilized to control the reaction pH. All of the utilized chemicals were ordered from Sigma-Aldrich Company and utilized as attained. The preparation process of NiO NPs was as the following. 50 mL of *Rhus coriaria* extract was used and added dropwise to 50 mL of Nickel nitrate solution under magnetic stirring at 70 °C for 30 min. In addition, the pH was controlled up to 10 of the mixture by adding sodium hydroxide (NaOH) until the colour of the solution was changed to a black colour, which means that the reaction started with the nucleation and growth process of the NiO NPs. The obtained precipitate nanoparticles were separated from the solution by centrifugation at 7000 rpm for 30 min and subsequently heated at 500 °C for 2 h using a muffle oven to remove all of the impurities and organic materials around the NiO NPs. Then, the nanoparticles were checked by UV–Vis spectrometer.

2.3.2 Preparation of Ag nanoparticles

As stated previously, this study intended to produce Ag NPs using green synthesis method. *Rhus coriaria* extract employed as a reducing, capping, and stabilizing agents and silver nitrate, $AgNO_3$, utilized as an Ag ion source. In addition, sodium hydroxide, NaOH, utilized to control the reaction pH. All of the employed chemicals were ordered from Sigma-Aldrich Company and employed as achieved. The preparation process of Ag NPs was as the following. The amount of 2 mg of silver nitrite was dissolved using ultrasonication in 50 mL double distilled water and put on the magnetic stirrer hot plate at 70 °C for 30 min. Then, 50 mL of *Rhus coriaria* extract solution was dropwise added to the dissolved silver nitrite solution until the colour of the mixture changed to a brownish colour (Fig. 1). The new appearance of the mixture is considered an indicator for synthesizing Ag NPs; afterwards, the nanoparticles were confirmed by UV–Vis double beam spectroscopy. The obtained precipitate nanoparticles were separated from the solution by centrifugation at 7000 rpm for 30 min and subsequently heated at 500 °C for 2 h using a muffle oven to remove all of the impurities and organic materials around the Ag NPs.

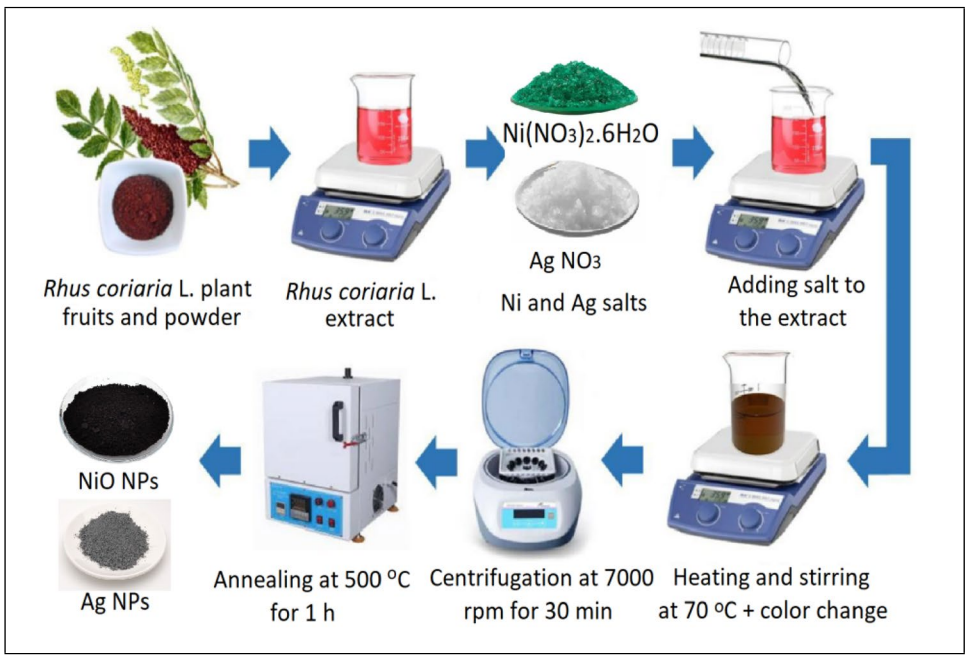

Fig. 1 Schematic diagram for the green synthesis of NiO and Ag NPs

2.4 Treatment of parasites with nanoparticles

2.4.1 Collection of nematodes

The adult nematodes (males and females) were collected from freshly slaughtered goats at Soran abattoir as follows: The abomasums of slaughtered goats were put in plastic bags and transferred quickly to the laboratory of the Biogeosciences department in Scientific Research Center of Soran University. Subsequently, they were washed carefully and thoroughly by normal saline and the adult worms were collected and identified at magnification 400 × and 100 × using previously described identification keys (Taylor, Coop, & Wall, 2015). Then, the *Marshallagia marshalli* nematodes were separated and preserved in Phosphate Buffered Saline (PBS) solution (pH = 7.4) at 37 ± 2 °C for further analysis.

2.4.2 Preparation of nanoparticle suspensions

Nickel oxide and silver nanoparticles were separately suspended in PBS solution. The produced agglomeration was broken by intermittent sonication using a sonicator probe at 30 W for 10 min. The final concentrations of 1, 2, 4, 8, 12, and 16 ppm were prepared based on a previously described procedure [39].

2.4.3 Evaluation of parasite motility

Each prepared concentration of nanoparticles (the final volume 50 mL) was poured into a sterile petri dish and twenty motile nematodes were placed in petri dishes. The petri dishes contained only PBS solution and motile worms were added as a negative control. The motility of nematodes for each concentration of every type of nanoparticles (nickel oxide and silver) was evaluated and recorded at every 4-h interval up to 24 h (Tables 1 and 2). The experiment was carried out with three replicates.

2.4.4 Assessment of egg hatching ability

Adult female of *M. marshalli* were used as a source of fresh eggs. Collection of eggs and the egg hatch test (EHT) was carried out according to Coles et al. [40] and Hubert and Kerboeuf, [41] with some modifications as follows:

The alive and fresh *M. marshalli* females (50 nematodes) were crushed in a container containing 100 mL of PBS solution; then, the contents were mixed, thoroughly homogenized and filtered through the sieve (No. 100). The sieved content was collected, divided into Clayton Lane tubes and centrifuged (2000 rpm for 10 min). Then, the supernatant solution was gently poured and discarded. After agitating, mixing and suspending of content, the magnesium sulphate solution (specific gravity: 1.25) was added to the sediment remaining in each centrifuge tube until a meniscus formed above the tube. A coverslip was added to each tube and centrifuged at 1500 rpm for 10 min. The coverslips were carefully picked off and washed with PBS solution into a conical glass centrifuge tube. Then, they were washed three times with PBS solution. In order to prevent damage to the eggs, all experiment steps were performed immediately. Finally, a suspension containing approximately 200 g eggs/mL in PBS was prepared and used for the experiment.

Table 1 The motility of *M. marshalli* after exposure to various concentrations of Ag-NPs in different incubation times

	Control	1 ppm	2 ppm	4 ppm	8 ppm	12 ppm	16 ppm
4 h	+ + + +	+ + + +	+ + + +	+ + + +	+ + + +	+ + +	+ + +
8 h	+ + + +	+ + + +	+ + + +	+ + + +	+ + + +	+ + +	+ + +
12 h	+ + + +	+ + + +	+ + + +	+ + + +	+ + +	+ + +	+ +
16 h	+ + + +	+ + + +	+ + + +	+ + +	+ + +	+ +	+
20 h	+ + + +	+ + + +	+ + +	+ +	+ +	+	-
24 h	+ + +	+ + +	+ +	+	-	-	-

High: + + + +, moderate: + + +, low: + +, very low: +, no motility: -

Table 2 The motility of *M. marshalli* after exposure to the different concentrations of NiO-NPs in various incubation times

	Control	1 ppm	2 ppm	4 ppm	8 ppm	12 ppm	16 ppm
4 h	+ + + +	+ + + +	+ + + +	+ + + +	+ + + +	+ + + +	+ + + +
8 h	+ + + +	+ + + +	+ + + +	+ + + +	+ + + +	+ + + +	+ + + +
12 h	+ + + +	+ + + +	+ + + +	+ + + +	+ + + +	+ + + +	+ + +
16 h	+ + + +	+ + + +	+ + + +	+ + + +	+ + + +	+ + +	+ + +
20 h	+ + + +	+ + + +	+ + + +	+ + + +	+ + +	+ +	+
24 h	+ + +	+ + +	+ + +	+ + +	+ +	+	-

Highs: + + + +, moderate: + + +, low: + +, very low: +, no motility: -

Different concentrations of 1, 2, 4, 8, 12, and 16 ppm of nanoparticles were poured into the wells of a 24 well plate. Then, 100 µl of fresh egg suspension were added to each well. PBS solution was used as a negative control. The eggs were kept at 22–24° C in incubator. The experiment was carried out with three replicates for each type of nanoparticle. After 24 h, the experiment was terminated by adding 10 ml of Lugol's iodine to each well and the hatched (L1) and unhatched eggs were counted under the light microscope. Finally, the mean percentage of hatching for three replicates was calculated for each concentration.

2.4.5 Statistical analysis

The results of egg hatching were analyzed using (one-way ANOVA) followed by means treatment/Duncan test ($P < 0.05$) for comparing the mean of hatching in different concentrations of each type of nanoparticles (utilizing the SAS 9.1 program). Moreover, a *T*-test ($P < 0.05$) was performed in order to compare the mean percentage of egg hatching in the same concentrations of two types of nanoparticles (Table 3).

3 Results and discussion

3.1 UV–Vis spectrum of the Rhus coriaria extract

Figure 2 shows the UV–Vis spectrum of *Rhus coriaria* extraction, the peak at 264 nm is corresponding to the methyl gallate which is a strong antioxidant phenolic compound [42]. The available bioactive molecules in the *Rhus coriaria* extract, precisely methyl gallate possesses several OH groups [43], that behaves as a reducing, capping, and stabilizing agent for the growth of NiO and Ag nanoparticles. The UV–Vis absorption band was related to the main component i.e. flavonoids. Barzinjy et al. [44] utilized *Rhus coriaria* extraction for synthesizing iron oxide NPs; they found that the available antioxidants inside the extraction are capable of producing uniform Fe_3O_4 NPs.

Table 3 The mean percentage of egg hatching after exposure to various concentrations of examined nanoparticles (mean of 3 replications)

Concentration	Ag-NPs (±SD)	NiO-NPs (±SD)
Control	57.9Aa (±0.69)	61.167Aa (±3.75)
1 ppm	59.367Aa (±6.64)	60.067Aa (±2.54)
2 ppm	43Ab (±3.64)	50.633Ab (±5.7)
4 ppm	39.133Ab (±2.05)	44.783Abc (±1.42)
8 ppm	30.533Bc (±0.86)	44.133Ac (±0.61)
12 ppm	21.967Bd (±2.57)	42.333Ac (±0.32)
16 ppm	17.2Bd (±2.08)	32.2Ad (±0.1.55)

Lowercase letters compare the mean in the columns while capital letters compare the mean in the rows. Different letters indicate significantly different values ($p < 0.05$).

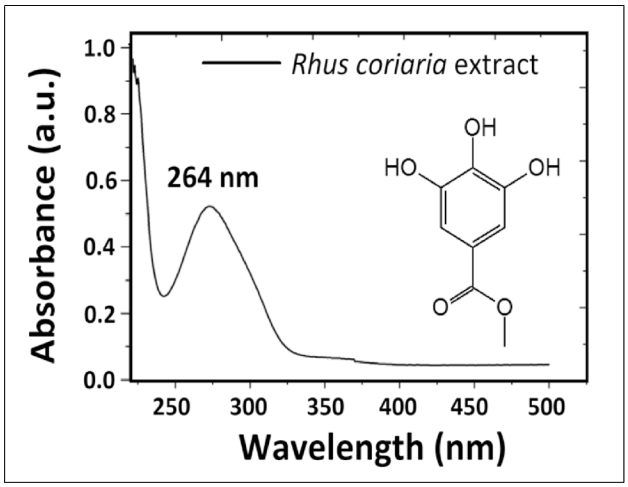

Fig. 2 UV–Vis absorption spectrum of *Rhus coriaria* extract

3.2 UV–Vis spectrum of the biosynthesized NiO and Ag NPs

To investigate the optical properties of the green synthesized NiO NPs, UV–Vis absorption spectra was documented as displayed in Fig. 3a. The UV–Vis spectroscopy shows an absorption peak at 350 nm, in the UV region indicating the formation of NiO NPs. [45]. This blue-shifted observation compared to the bulk NiO materials is accredited to the quantum confinement effect [46]. In another story of Fig. 3a, there are no additional peaks related to the impurities and defects which is a good indication for the high quality of crystalline synthesized NiO NPs. The UV–Vis absorption spectrum as presented in Fig. 3b revealed the formation of Ag NPs, which is located in the visible spectrum of 445 nm. Moreover, the conduction and valence bands of Ag NPs are very close to each other, allowing that the free electrons might have oscillation between these two bands producing the surface plasmon resonance (SPR) phenomena, this agreed with both studies from Yallappa et al. [47] and Ashraf et al. [48]. The absence of additional peaks in the UV–Vis range is a good indicator of the purity of the fabricated Ag NPs. The results of this study are in agreement with the previous works, showing that the SPR peaks for the Ag NPs typically appears between 410 and 480 nm [49, 50].

3.3 X-ray diffraction (XRD) of the green synthesized NiO and Ag NPs

As shown in Fig. 4a, synthetic NiO NPs were examined between 20 and 80 θ–2θ degrees using XRD technique. The

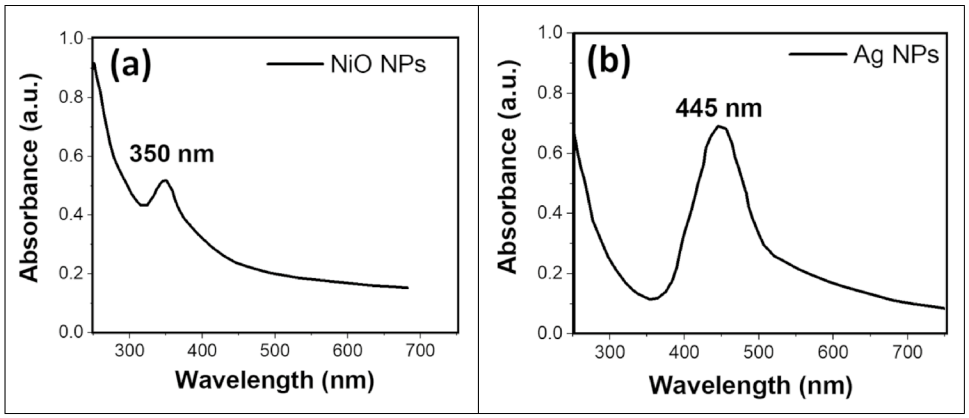

Fig. 3 UV–Vis spectra of **a** NiO NPs, **b** Ag NPs prepared by *Rhus coriaria* extract

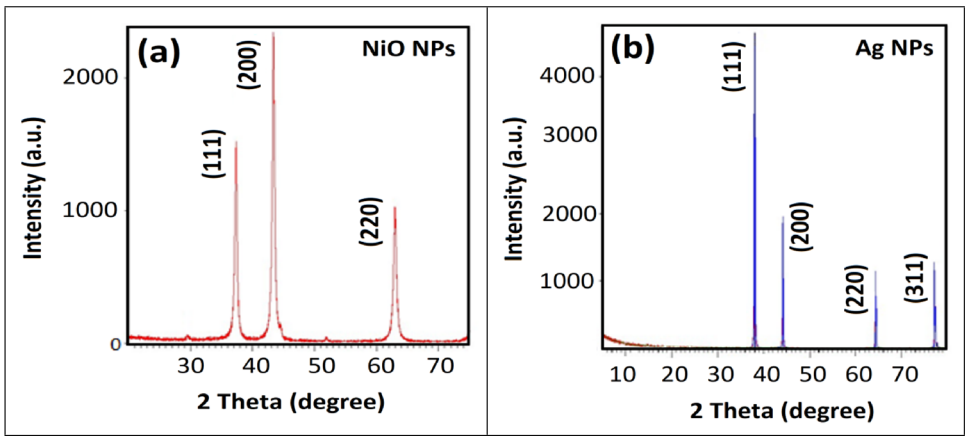

Fig. 4 XRD spectra of **a** NiO NPs, **b** Ag NPs prepared by *Rhus coriaria* extract

crystal structure of the green produced NiO NPs was confirmed by this XRD spectrum from. It is possible to identify the planes (111), (200), and (220) by their peak positions at 37.24, 43.26, and 62.84 degrees accordingly. Rendering to the prior research, these peaks are in concordance with [34–36, 51]. The spectrum shows that all the peaks were in agreement with the regular (JSPDS Card no. 65–2901) with $a=b=c=4.197$ A°. Therefore, there is no extra peak in the XRD pattern, which is a favorable sign that no impurity peaks have been found. The Debye–Scherrer equation is used to calculate the average crystallite size from the XRD data.

$$D = \frac{0.95\lambda}{\beta_D \cos\theta} \tag{1}$$

where D is the average crystallite size, λ is the wavelength of the X-ray (0.154 nm), θ is the Bragg's angle, and β_D is full width at half maximum (FWHM) which it is almost equal to ~ 0.2475 calculated from (200) plane. According to the calculation above, the average crystallite size computed is around 35 nm for NiO NPs. There is good agreement between the obtained crystal structure of NiO NPs and the prior studies [52].

Figure 4b depicts the XRD pattern of the fabricated Ag NPs. The crystalline structure of the Ag NPs is seen in this pattern. The (111), (200), (220), and (311) planes correspond to the peaks at 38.01°, 44.34°, 65.52°, and 77.30°, respectively. According to the earlier investigations, these peaks can be attributed to the face-centered cubic structure of Ag nanostructures [53, 54]. Also, Fig. 4b shows that the diffraction pattern has been matched with JCPDS card No. 65–2901 and all the diffraction peaks were indexed to the pure cubic Ag structure. It is clear from the XRD patterns that the Ag NPs created from plant extract are exceptionally pure. In contrast to other fabrication processes, the green synthesis method produces pure, high-quality, and stable Ag NPs [55]. Using the Debye–Scherer formula, the average crystallite size of Ag NPs is approximately 40 nm.

3.4 FE-SEM analysis from green synthesized NiO and Ag NPs

The surface morphology of synthesized NiO nanoparticles has been studied by the field emission scanning electron microscope FE-SEM, as depicted in Fig. 5a. It is clear from the Fig. 5a that the grown NiO NPs are agglomerated and almost all of the NiO NPs possess a spherical shape with

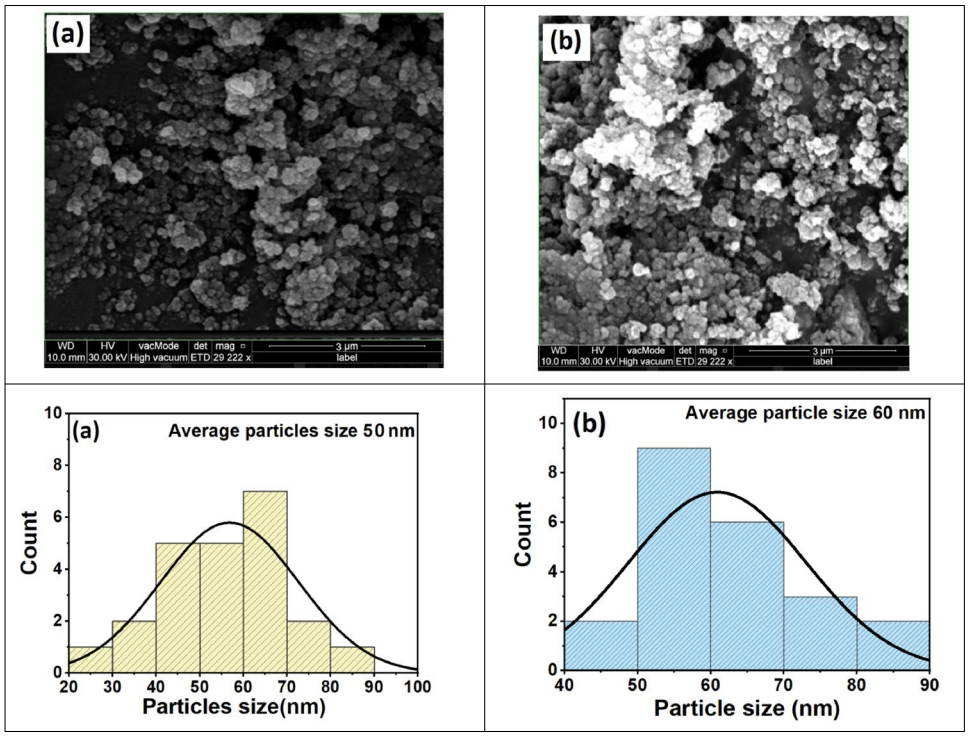

Fig. 5 Top view morphology of biosynthesized NiO NPs (**a**) and Ag NPs (**b**) along with their corresponding particle size distributions

an average diameter was about 50 nm. The agglomeration is generally due to a high surface area per unit volume ratio and capping agents such as enzyme, protein, vitamin, and polyphenols from the phytochemical species of plant extraction. Also, the NiO NPs are not analogous in shape and size, which could be initiated from the non-uniform nucleation and growth process.

Moreover, the morphology and size of green synthesized Ag nanoparticles were characterized using FE-SEM analysis, as can be seen from Fig. 5b. The Ag NPs were in the nanometer range and the particles have a spherical shape with some agglomerations of nanoparticles and the average size diameter was about 60 nm.

3.5 EDX measurements from green synthesized NiO and Ag NPs

The elemental composition of the produced NiO and Ag NPs by the green method was studied through energy dispersive X-ray (EDX) analysis highlighted in Fig. 6. EDX spectra displayed a strong signal from the Ni atoms at 7.5 keV and O atoms at 0.5 keV as clear from Fig. 6a, which confirmed the formation of NiO NPs and their elemental nature. However, Fig. 6a shows the pure synthesized NiO samples without impurity from the other elements. Figure 6b shows that the sample contained Ag as an essential element with no impurity from other elements. The signals from gold (Au) were

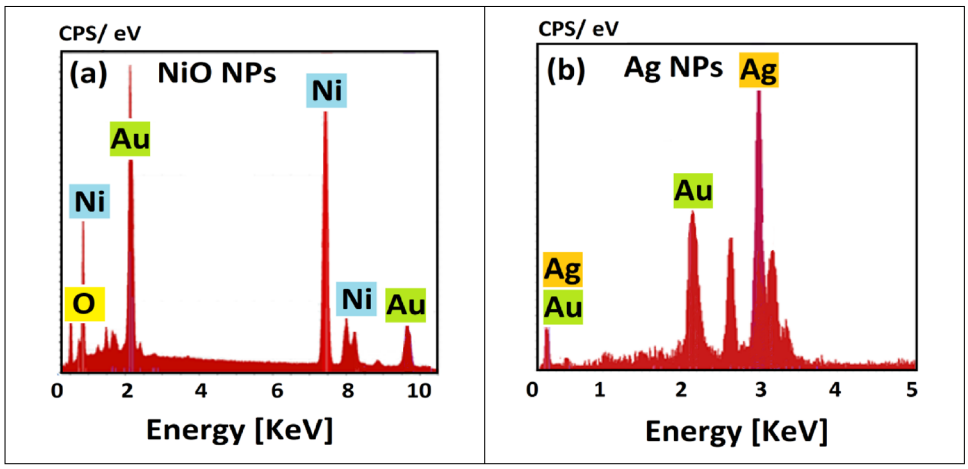

Fig. 6 EDX analysis of biosynthesized **a** NiO NPs and **b** Ag NPs by *Rhus coriaria* extract

detected in Fig. 6, related to the coating of the NiO and Ag NPs samples with a 250 Å layer of Au to enhance the resolution of the SEM images. A similar study has been found by Ahani and Khatibzadeh [56].

3.6 Effect of nanoparticles of motility and egg hatching ability

Adult male and female of *M. marshalli* nematodes were identified morphologically (Fig. 7). The motility of the worms reduced as the concentration of nanoparticles and the length of incubation increased, to the point where no movement in the worms was seen after 24 h at the highest concentration (16 ppm). However, most nematodes were still motile in low concentrations and control until the endpoint.

Immobility in Trichostrongylid nematodes is a sign of death [57] and clearly indicates the effect of examined compounds on *M. marshalli.* According to prior research, nanoparticles, particularly AgNPs, have negative effects on gastrointestinal nematodes [58, 59]. Also collected evidence that supports our findings that low concentrations of Ag NPs reduced worm movement, emphasizing the stronger anthelmintic activity of Ag NPs compared to NiO NPs [60].

The higher antiparasitic properties activity of Ag NPs were also observed in the next stage of the experiment where only 17.2% of eggs hatched after 24 h incubation in a 16 ppm concentration of Ag NPs ($p < 0.05$) (Fig. 8).

It can be seen from Table 3 that the mean percentage of egg hatching in controls was 57.9 and 61.1 for Ag NPs and NiO NPs respectively without significant differences at the level of 95% confidence intervals ($p > 0.05$). However, after increasing concentration, particularly in Ag NPs, the ovicidal activity was significantly and respectively observed especially in (4, 8, and 12 ppm) while no significant differences were detected in the same concentrations of NiO NPs. Comparing the same concentrations of nanoparticles together also showed that until 4 ppm concentration, the ovicidal activity is not significantly different and two types of compounds have the same activity on the eggs but other concentrations (8, 12, and 16 ppm) showed significant levels of inhibition, and despite the differences in comparison to control, Ag NPs were more effective than NiO NPs. Nanoparticles have their specific physical, chemical, and biological properties; they may also be different size and surface area. Moreover, many types of nanoparticles have the ability to damage cells through different pathways; thus, these

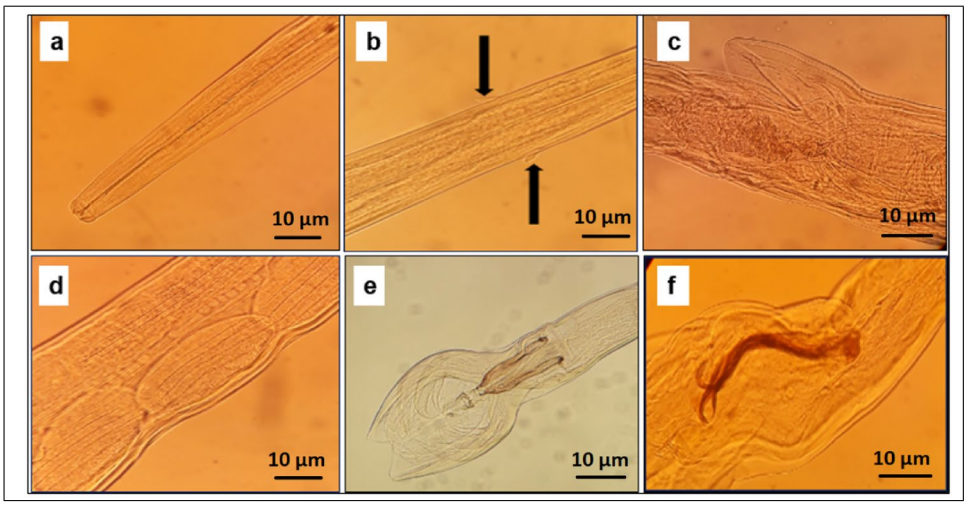

Fig. 7 Various parts of detected *M. marshalli*: **a** small head and buccal cavity, **b** the tiny cervical papillae on the anterior end of both sexes (arrows), **c** in females, a vulvar flap can be present, **d** ellipsoidal eggs in the body of the female worm, **e** copulatory bursa and spicules, **f** three small process of spicule in the adult male of *M. marshalli* (lateral view of copulatory bursa)

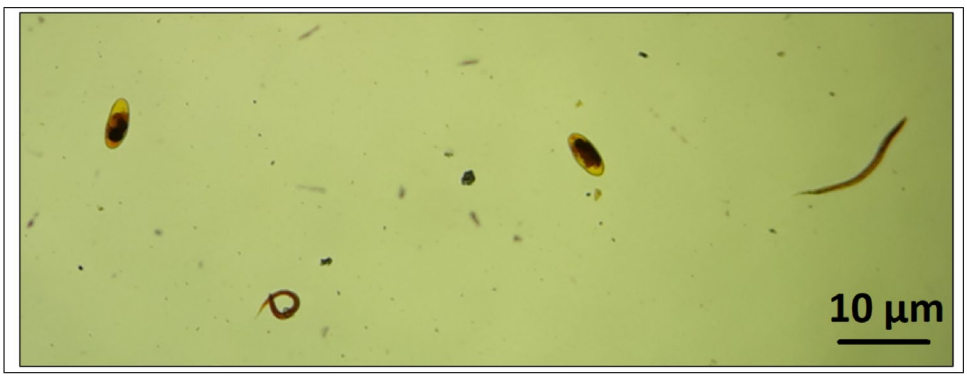

Fig. 8 The hatched (larvae) and unhatched eggs of *M. marshalli* after exposure to the nanoparticles

factors may affect their efficiency as an anthelmintic agent. Suresh et al. [61] studied NiO NPs as antibacterial and antifungal activities; they confirmed the improved effect of NiO nanoparticles which might be due to enhanced dispersibility and interaction of NiO NPs with membrane and intracellular proteins of bacteria and fungi. Esmaielnejad et al. (2018) reported that ZnO-NPs exert remarkable anthelmintic effects via induction of oxidative/nitrosative stress and DNA damage. Marimuthu et al. [62] investigated the assessments of the antiparasitic pursues to determine the abilities of green synthesized silver nanoparticles against the larvae parasite, which had been exposed to different concentrations of Ag NPs for 24 h. They showed the green synthesized Ag NPs are stable and had important mosquito larvicidal activity. Another study indicated that green synthesized ZnO NPs had the best scolicidal activity at 400 ppm concentration after 150 min of exposure time, displaying 100% mortality rate. The treated protoscolices revealed loss of viability with numerous morphological alterations [63].

Regarding egg hatching in *M. marshalli*, Taylor et al. [64] suggested that hatching occurs as L2 with the first moult occurring inside the egg. However, recent studies demonstrated that environmental factors especially the temperature are associated with larval stage, development of larvae in the egg and timing of hatching [11, 12, 65]. In the present study, the eggs were kept at 22–24 °C and the L1 were the most of hatched larvae. This is in agreement with Aleuy et al. [65] who showed that most of cultured eggs at 20° C were hatched as L1s and hatching as an L3 were occurred at higher incubation temperatures.

Although the egg hatching ability in our study was assessed for 24 h, the low hatching percentage in the control groups indicated that the longer period times of incubation probably increase the chance of hatching and should be considered in future studies. Moreover, previous studies revealed that in response to the unsuitable environmental conditions, *M. marshalli* represent different hatching behaviour [11, 12, 65, 66]. Our findings indicated that Ag NPs and NiO NPs especially AgNPs have negative and lethal effects on *M. marshalli* and the presence of such materials as an unfavorable factor suppressed the hatching process; however, the possible changes in the morphology of the eggs and larvae within the eggs, stages of larvae during the different period times of incubation, and the number of replicates and sample size in experiment deserve further consideration [34–36].

4 Conclusion

In this investigation, NiO and Ag NPs were produced effectively through a green method utilizing *Rhus coriaria* extract, as a reducing, capping and stabilizing agents. Numerous characterization techniques have been employed to study the morphology, pureness, degree of crystallinity, structural, and optical properties of the biosynthesized NiO and Ag NPs. Taken together, the results of the present study show that the NiO and Ag NPs have anthelmintic effects on *M. marshalli* as one of the important nematodes in small ruminants. Furthermore, the effects of these nanoparticles depend on concentration and time of exposure or incubation. In addition, Ag NPs have more efficiency and activity on mentioned nematode compared to NiO NPs. Future studies should focus on ultrastructural changes and sites of effect in nematodes after exposure to nanoparticles, appropriate concentrations, in vivo efficacy of nanoparticles on gastrointestinal nematodes and side effects on hosts of nematodes. Also, different metal and metal oxide NPs can be tested to investigate the anthelmintic effects on *M. marshalli* and other parasite of ruminants.

Acknowledgements and the authors would like to thank the scientific research centre (SRC) at Soran University, Sisaf Nanotechnology Drug Delivery, Ulster University for their support.

Declarations

Ethics approval Not applicable.

Conflict of interest The authors declare no competing interests.

Open Access This article is licensed under a Creative Commons Attribution 4.0 International License, which permits use, sharing, adaptation, distribution and reproduction in any medium or format, as long as you give appropriate credit to the original author(s) and the source, provide a link to the Creative Commons licence, and indicate if changes were made. The images or other third party material in this article are included in the article's Creative Commons licence, unless indicated otherwise in a credit line to the material. If material is not included in the article's Creative Commons licence and your intended use is not permitted by statutory regulation or exceeds the permitted use, you will need to obtain permission directly from the copyright holder. To view a copy of this licence, visit http://creativecommons.org/licenses/by/4.0/.

References

1. Rehman, A., Abidi, S. (2022). Livestock health: current status of helminth infections and their control for sustainable development. In Advances in Animal Experimentation and Modeling (pp. 365–378): Elsevier. https://doi.org/10.1016/B978-0-323-90583-1.00029-5
2. Morand, S., Bouamer, S., Hugot, J.-P. (2006). Nematodes. In Micromammals and Macroparasites (pp. 63–79): Springer. https://doi.org/10.1007/978-4-431-36025-4_4
3. F. Roeber, A.R. Jex, R.B. Gasser, Impact of gastrointestinal parasitic nematodes of sheep, and the role of advanced molecular tools for exploring epidemiology and drug resistance-an Australian perspective. Parasit. Vectors **6**, 1–13 (2013). https://doi.org/10.1186/1756-3305-6-153
4. O.A. Aleuy, K. Ruckstuhl, E.P. Hoberg, A. Veitch, N. Simmons, S.J. Kutz, Diversity of gastrointestinal helminths in Dall's sheep

and the negative association of the abomasal nematode, Marshallagia marshalli, with fitness indicators. PLoS ONE **13**, 1–21 (2018). https://doi.org/10.1371/journal.pone.0192825
5. Barghandan, T., Hajialilo, E., Sharifdini, M., and Javadi, A., (2019), Prevalence and phylogenetic analysis of gastrointestinal helminths (Nematoda: Trichostrongylidae) in ruminant livestock of northwest Iran. *Ankara Üniversitesi Veteriner Fakültesi Dergisi,* 67 pp. 65–72. https://doi.org/10.33988/auvfd.588539
6. A. Carlsson, R.J. Irvine, K. Wilson, S.B. Piertney, O. Halvorsen, S.J. Coulson, A. Stien, S.D. Albon, Disease transmission in an extreme environment: nematode parasites infect reindeer during the Arctic winter. Int. J. Parasitol. **42**, 789–795 (2012). https://doi.org/10.1016/j.ijpara.2012.05.007
7. H. Hosseinnezhad, M. Sharifdini, K. Ashrafi, Z. Atrkar Roushan, H. Mirjalali, B. Rahmati, Trichostrongyloid nematodes in ruminants of northern Iran: prevalence and molecular analysis. BMC Vet. Res. **17**, 1–12 (2021). https://doi.org/10.1186/s12917-021-03086-3
8. I. Zouyed, J. Cabaret, B. Bentounsi, Climate influences assemblages of abomasal nematodes of sheep on steppe pastures in the east of Algeria. J. Helminthol. **92**, 34–41 (2018). https://doi.org/10.1017/S0022149X16000845
9. A. Kuchboev, K. Sobirova, R. Karimova, O. Amirov, G. von Samson-Himmelstjerna, J. Krücken, Molecular analysis of polymorphic species of the genus Marshallagia (Nematoda: Ostertagiinae). Parasit. Vectors **13**, 1–12 (2020). https://doi.org/10.1186/s13071-020-04265-1
10. N. Moradpour, H. Borji, G. Razmi, M. Maleki, H. Kazemi, Pathophysiology of Marshallagia marshalli in experimentally infected lambs. Parasitology **140**, 1762–1767 (2013). https://doi.org/10.1017/S0031182013001042
11. O.A. Aleuy, S. Peacock, E.P. Hoberg, K.E. Ruckstuhl, T. Brooks, M. Aranas, S. Kutz, Phenotypic plasticity and local adaptation in freeze tolerance: Implications for parasite dynamics in a changing *world*. Int. J. Parasitol. **50**, 161–169 (2020). https://doi.org/10.1016/j.ijpara.2019.12.004
12. O.A. Aleuy, E. Serrano, K.E. Ruckstuhl, E.P. Hoberg, S. Kutz, Parasite intensity drives fetal development and sex allocation in a wild ungulate. Sci. Rep. **10**, 1–10 (2020). https://doi.org/10.1038/s41598-020-72376-x
13. A.S. Cezar, G. Toscan, G. Camillo, L.A. Sangioni, H.O. Ribas, F.S.F. Vogel, Multiple resistance of gastrointestinal nematodes to nine different drugs in a sheep flock in southern Brazil. Vet. Parasitol. **173**, 157–160 (2010). https://doi.org/10.1016/j.vetpar.2010.06.013
14. N. George, K. Persad, R. Sagam, V. Offiah, A. Adesiyun, W. Harewood, N. Lambie, A. Basu, Efficacy of commonly used anthelmintics: First report of multiple drug resistance in gastrointestinal nematodes of sheep in Trinidad. Vet. Parasitol. **183**, 194–197 (2011). https://doi.org/10.1016/j.vetpar.2011.06.014
15. D. Traversa, B. Paoletti, D. Otranto, J. Miller, First report of multiple drug resistance in trichostrongyles affecting sheep under field conditions in Italy. Parasitol. Res. **101**, 1713–1716 (2007). https://doi.org/10.1007/s00436-007-0707-4
16. D. Gottschall, V. Theodorides, R. Wang, The metabolism of benzimidazole anthelmintics. Parasitol. Today **6**, 115–124 (1990). https://doi.org/10.1016/0169-4758(90)90228-V
17. C.E. Lanusse, R.K. Prichard, Clinical pharmacokinetics and metabolism of benzimidazole anthelmintics in ruminants. Drug Metab. Rev. **25**, 235–279 (1993). https://doi.org/10.3109/03602539308993977
18. A. El-makawy, H.A. Radwan, I.S. Ghaly, A. Abdelraouf, Genotoxical, teratological and biochemical effects of anthelmintic drug oxfendazole Maximum Residue Limit (MRL) in male and female mice. Reprod. Nutr. Dev. **46**, 139–156 (2006)
19. Q. Mckellar, Ecotoxicology and residues of anthelmintic compounds. Vet. Parasitol. **72**, 413–435 (1997). https://doi.org/10.1016/S0304-4017(97)00108-8
20. Sabouri, Z., Rangrazi, A., Amiri, M.S., Khatami, M. and Darroudi, M., (2021), Green synthesis of nickel oxide nanoparticles using Salvia hispanica L.(chia) seeds extract and studies of their photocatalytic activity and cytotoxicity effects. *Bioprocess and Biosystems Engineering*, *44*(11), pp.2407–2415. https://doi.org/10.1007/s00449-021-02613-8
21. Z. Sabouri, A. Akbari, H.A. Hosseini, M. Khatami, M. Darroudi, Green-based bio-synthesis of nickel oxide nanoparticles in Arabic gum and examination of their cytotoxicity, photocatalytic and antibacterial effects. Green Chem. Lett. Rev. **14**(2), 404–414 (2021). https://doi.org/10.1080/17518253.2021.1923824
22. H.U.R. Bajwa, M.K. Khan, Z. Abbas, R. Riaz, R.Z. Abbas, M.T. Aleem, A. Asghar, M.A. Almutairi, F.A. Alshammari, Y. Alraey, A. Alouffi, Nanoparticles: Synthesis and their role as potential drug candidates for the treatment of parasitic diseases. Life **12**, 1–16 (2022). https://doi.org/10.3390/life12050750
23. V. Wagner, A. Dullaart, A.-K. Bock, A. Zweck, The emerging nanomedicine landscape. Nat. Biotechnol. **24**, 1211–1217 (2006). https://doi.org/10.1038/nbt1006-1211
24. A. Chen, Y. Shi, Z. Yan, H. Hao, Y. Zhang, J. Zhong, H. Hou, Dosage form developments of nanosuspension drug delivery system for oral administration route. Curr. Pharm. Des. **21**, 4355–4365 (2015). https://doi.org/10.2174/1381612821666150901105026
25. M. Hamori, S. Yoshimatsu, Y. Hukuchi, Y. Shimizu, K. Fukushima, N. Sugioka, A. Nishimura, N. Shibata, Preparation and pharmaceutical evaluation of nano-fiber matrix supported drug delivery system using the solvent-based electrospinning method. Int. J. Pharm. **464**, 243–251 (2014). https://doi.org/10.1016/j.ijpharm.2013.12.036
26. Y. Xu, X. Zhong, X. Zhang, W. Lv, J. Yu, Y. Xiao, S. Liu, J. Huang, Preparation of intravenous injection nanoformulation via co-assemble between cholesterylated gemcitabine and cholesterylated mPEG: enhanced cellular uptake and intracellular drug-controlled release. J. Microencapsul. **34**, 185–194 (2017). https://doi.org/10.1080/02652048.2017.1316323
27. Z.-H. Zhang, Y.-L. Zhang, J.-P. Zhou, H.-X. Lv, Solid lipid nanoparticles modified with stearic acid–octaarginine for oral administration of insulin. Int. J. Nanomed. **7**, 3333–3339 (2012). https://doi.org/10.2147/IJN.S31711
28. S. Das, A. Chaudhury, Recent advances in lipid nanoparticle formulations with solid matrix for oral drug delivery. AAPS PharmSciTech **12**, 62–76 (2011). https://doi.org/10.1208/s12249-010-9563-0
29. J.S. Negi, P. Chattopadhyay, A.K. Sharma, V. Ram, Development of solid lipid nanoparticles (SLNs) of lopinavir using hot self nano-emulsification (SNE) technique. Eur. J. Pharm. Sci. **48**, 231–239 (2013). https://doi.org/10.1016/j.ejps.2012.10.022
30. W.C. Chan, S. Nie, Quantum dot bioconjugates for ultrasensitive nonisotopic detection. Science **281**, 2016–2018 (1998). https://doi.org/10.1126/science.281.5385.2016
31. L. Mazzola, Commercializing nanotechnology. Nat. Biotechnol. **21**, 1137–1143 (2003). https://doi.org/10.1038/nbt1003-1137
32. Ramsden, J. (2016) Nanotechnology: An introduction: 2nd Edition William Andrew. https://www.elsevier.com/books/nanotechnology/ramsden/978-0-323-39311-9
33. S. Faisal, N.S. Al-Radadi, H. Jan, S.A. Shah, S. Shah, M. Rizwan, Z. Afsheen, Z. Hussain, U.N. Nazir, N. Idrees, N. Bibi, Curcuma longa mediated synthesis of copper oxide, nickel oxide and Cu-Ni bimetallic hybrid nanoparticles: Characterization and evaluation for antimicrobial, anti-parasitic and cytotoxic potentials. Coatings **11**, 849 (2021). https://doi.org/10.3390/coatings11070849

34. Z. Sabouri, A. Akbari, H.A. Hosseini, M. Khatami, M. Darroudi, Tragacanth-mediate synthesis of NiO nanosheets for cytotoxicity and photocatalytic degradation of organic dyes. Bioprocess Biosyst. Eng. **43**(7), 1209–1218 (2020). https://doi.org/10.1007/s00449-020-02315-7
35. Z. Sabouri, N. Fereydouni, A. Akbari, H.A. Hosseini, A. Hashemzadeh, M.S. Amiri, R. Kazemi Oskuee, M. Darroudi, Plant-based synthesis of NiO nanoparticles using salvia macrosiphon Boiss extract and examination of their water treatment. Rare Met. **39**(10), 1134–1144 (2020). https://doi.org/10.1007/s12598-019-01333-z
36. Z. Sabouri, A. Akbari, H.A. Hosseini, M. Khatami, M. Darroudi, Egg white-mediated green synthesis of NiO nanoparticles and study of their cytotoxicity and photocatalytic activity. Polyhedron **178**, 114351 (2020). https://doi.org/10.1016/j.poly.2020.114351
37. Z. Baghbani, B. Esmaeilnejad, S. Asri-Rezaei, Assessment of oxidative/nitrosative stress biomarkers and DNA damage in Teladorsagia circumcincta following exposure to zinc oxide nanoparticles. J. Helminthol. **94**, 115 (2020). https://doi.org/10.1017/S0022149X19001068
38. M. Adeel, C. Ma, S. Ullah, M. Rizwan, Y. Hao, C. Chen, G. Jilani, N. Shakoor, M. Li, L. Wang, D.C. Tsang, J. Rinklebehi, Y. Ruia, B. Xingc, Exposure to nickel oxide nanoparticles insinuates physiological, ultrastructural and oxidative damage: A life cycle study on Eisenia fetida. Environ. Pollut. **254**, 113032 (2019). https://doi.org/10.1016/j.envpol.2019.113032
39. B. Esmaeilnejad, A. Samiei, Y. Mirzaei, F. Farhang-Pajuh, Assessment of oxidative/nitrosative stress biomarkers and DNA damage in Haemonchus contortus, following exposure to zinc oxide nanoparticles. Acta Parasitol. **63**, 563–571 (2018). https://doi.org/10.1515/ap-2018-0065
40. G. Coles, C. Bauer, F. Borgsteede, S. Geerts, T. Klei, M. Taylor, P. Waller, World Association for the Advancement of Veterinary Parasitology (WAAVP) methods for the detection of anthelmintic resistance in nematodes of veterinary importance. Vet. Parasitol. **44**, 35–44 (1992). https://doi.org/10.1016/0304-4017(92)90141-U
41. Hubert, J., Kerboeuf, D., (1984), A new method for culture of larvae used in diagnosis of ruminant gastrointestinal strongylosis: Comparison with fecal cultures. *Canadian Journal of Comparative Medicine,* 48 pp. 63–71. https://www.ncbi.nlm.nih.gov/pmc/articles/PMC1236007/
42. A.M. Youssef Moustafa, A.I. Khodair, M.A. Saleh, Isolation, structural elucidation of flavonoid constituents from Leptadenia pyrotechnica and evaluation of their toxicity and antitumor activity. Pharm. Biol. **47**, 539–552 (2009). https://doi.org/10.1080/13880200902875065
43. Z.A. Elagbar, A.K. Shakya, L.M. Barhoumi, H.I. Al-jaber, Phytochemical diversity and pharmacological properties of Rhus coriaria. Chem. Biodivers. **17**, 1–17 (2020). https://doi.org/10.1002/cbdv.201900561
44. A.A. Barzinjy, S.M. Hamad, S. Aydın, M.H. Ahmed, F.H. Hussain, Green and eco-friendly synthesis of Nickel oxide nanoparticles and its photocatalytic activity for methyl orange degradation. J. Mater. Sci.: Mater. Electron. **31**, 11303–11316 (2020). https://doi.org/10.1007/s10854-020-03679-y
45. A. Rahdar, M. Aliahmad, Y. Azizi, NiO nanoparticles: Synthesis and characterization. Journal of nanostructures **5**, 145–151 (2015). https://doi.org/10.7508/JNS.2015.02.009
46. G.A. Babu, G. Ravi, M. Navaneethan, M. Arivanandhan, Y. Hayakawa, An investigation of flower shaped NiO nanostructures by microwave and hydrothermal route. J. Mater. Sci.: Mater. Electron. **25**, 5231–5240 (2014). https://doi.org/10.1007/s10854-014-2293-4
47. S. Yallappa, J. Manjanna, S. Peethambar, A. Rajeshwara, N. Satyanarayan, Green synthesis of silver nanoparticles using Acacia farnesiana (Sweet Acacia) seed extract under microwave irradiation and their biological assessment. J. Cluster Sci. **24**, 1081–1092 (2013). https://doi.org/10.1007/s10876-013-0599-7
48. J.M. Ashraf, M.A. Ansari, H.M. Khan, M.A. Alzohairy, I. Choi, Green synthesis of silver nanoparticles and characterization of their inhibitory effects on AGEs formation using biophysical techniques. Sci. Rep. **6**, 1–10 (2016). https://doi.org/10.1038/srep20414
49. O. Kuntyi, A. Kytsya, I. Mertsalo, A. Mazur, G. Zozula, L. Bazylyak, R. Topchak, Electrochemical synthesis of silver nanoparticles by reversible current in solutions of sodium polyacrylate. Colloid Polym. Sci. **297**, 689–695 (2019). https://doi.org/10.1007/s00396-019-04488-4
50. A. Rahman, S. Kumar, A. Bafana, S.A. Dahoumane, C. Jeffryes, Biosynthetic conversion of Ag+ to highly stable Ag0 nanoparticles by wild type and cell wall deficient strains of Chlamydomonas reinhardtii. Molecules **24**, 98 (2019). https://doi.org/10.3390/molecules24010098
51. A. Barakat, M. Al-Noaimi, M. Suleiman, A.S. Aldwayyan, B. Hammouti, T.B. Hadda, S.F. Haddad, A. Boshaala, I. Warad, One step synthesis of NiO nanoparticles via solid-state thermal decomposition at low-temperature of novel aqua (2, 9-dimethyl-1, 10-phenanthroline) NiCl2 complex. Int. J. Mol. Sci. **14**, 23941–23954 (2013). https://doi.org/10.3390/ijms141223941
52. P. Kganyago, L. Mahlaule-Glory, M. Mathipa, B. Ntsendwana, N. Mketo, Z. Mbita, N.C. Hintsho-Mbita, Synthesis of NiO nanoparticles via a green route using Monsonia burkeana: the physical and biological properties. J. Photochem. Photobiol., B **182**, 18–26 (2018). https://doi.org/10.1016/j.jphotobiol.2018.03.016
53. M.H. Ahmed, T.E. Keyes, A.J. Byrne, C.J. Blackledge, J.W. Hamilton, Adsorption and photocatalytic degradation of human serum albumin on TiO2 and Ag-TiO2 films. J. Photochem. Photobiol. A Chem. **222**, 123–131 (2011). https://doi.org/10.1016/j.jphotochem.2011.05.011
54. M.H. Ahmed, T.E. Keyes, A.J. Byrne, The photocatalytic inactivation effect of Ag–TiO2 on β-amyloid peptide (1–42). J Photochem Photobiol, A **254**, 1–11 (2013). https://doi.org/10.1016/j.jphotochem.2012.12.019
55. S.S. Salem, A. Fouda, Green syntsshesis of metallic nanoparticles and their prospective biotechnological applications: an overview. Biol. Trace Elem. Res. **199**, 344–370 (2021). https://doi.org/10.1007/s12011-020-02138-3
56. M. Ahani, M. Khatibzadeh, Optimisation of significant parameters through response surface methodology in the synthesis of silver nanoparticles by chemical reduction method. Micro & Nano Letters **12**, 705–710 (2017). https://doi.org/10.1049/mnl.2017.0118
57. R.B. Elandalousi, H. Akkari, F. B'chir, M. Gharbi, M. Mhadhbi, S. Awadi, M.A. Darghouth, Thymus capitatus from Tunisian arid zone: Chemical composition and in vitro anthelmintic effects on Haemonchus contortus. Vet. Parasitol. **197**, 374–378 (2013). https://doi.org/10.1016/j.vetpar.2013.05.016
58. V. Goel, P. Kaur, L.D. Singla, D. Choudhury, Biomedical evaluation of Lansium parasiticum extract-protected silver nanoparticles against Haemonchus contortus, a parasitic worm. Front. Mol. Biosci. **7**, 396 (2020). https://doi.org/10.3389/fmolb.2020.595646
59. S. Preet, R.S. Tomar, Anthelmintic effect of biofabricated silver nanoparticles using Ziziphus jujuba leaf extract on nutritional status of Haemonchus contortus. Small Rumin. Res. **154**, 45–51 (2017). https://doi.org/10.1016/j.smallrumres.2017.07.002
60. N.K. Nasab, Z. Sabouri, S. Ghazal, M. Darroudi, Green-based synthesis of mixed-phase silver nanoparticles as an effective photocatalyst and investigation of their antibacterial properties. J. Mol. Struct. **1203**, 127411 (2020)
61. S. Suresh, S. Karthikeyan, P. Saravanan, K. Jayamoorthy, Comparison of antibacterial and antifungal activities of 5-amino-2-mercaptobenzimidazole and functionalized NiO nanoparticles.

Karbala International Journal of Modern Science **2**, 188–195 (2016). https://doi.org/10.1016/j.kijoms.2016.05.001
62. S. Marimuthu, Th. Santhoshkumar, A.V. Kirthi, Ch. Jayaseelan, A.Z. Bagavan, A.A. Zahir, G. Elango, Ch. Kamaraj, Evaluation of green synthesized silver nanoparticles against parasites. Parasitol Res **108**, 1541–1549 (2011). https://doi.org/10.1007/s00436-010-2212-4
63. Shnawa, B. H., Hamad, S. M., Barzinjy, A. A., Kareem, P. A., Ahmed, M. H., (2021), Scolicidal activity of biosynthesized zinc oxide nanoparticles by Mentha longifolia L. leaves against Echinococcus granulosus protoscolices. *Emergent Materials*, pp. 1–11. https://doi.org/10.1007/s42247-021-00264-9
64. Taylor, M. A., Coop, R., & Wall, R. L. (2015). Veterinary parasitology: John Wiley & Sons.
65. O.A. Aleuy, E.P. Hoberg, C. Paquette, K.E. Ruckstuhl, S. Kutz, Adaptations and phenotypic plasticity in developmental traits of Marshallagia marshalli. Int. J. Parasitol. **49**, 789–796 (2019). https://doi.org/10.1016/j.ijpara.2019.05.007
66. A. Carlsson, R. Irvine, K. Wilson, S. Coulson, Adaptations to the Arctic: low-temperature development and cold tolerance in the free-living stages of a parasitic nematode from Svalbard. Polar Biol. **36**, 997–1005 (2013). https://doi.org/10.1007/s00300-013-1323-7
67. M.G. Altas, M. Sevgili, A. Gokcen, N. Aksin, H.C. Bayburs, The prevalence of gastro-intestinal nematodes in hair goats of the Sanliurfa region. Turkiye Parazitolojii Dergisi **33**, 20–24 (2009). (**PMID: 19367541**)
68. H. De Ruyck, R. Van Renterghem, H. De Ridder, D. De Brabander, Determination of anthelmintic residues in milk by high performance liquid chromatography. Food Control **11**, 165–173 (2000). https://doi.org/10.1016/S0956-7135(99)00089-4
69. R. Iivine, A. Stien, O. Halvorsen, R. Langvatn, S. Albon, Life-history strategies and population dynamics of abomasal nematodes in Svalbard reindeer (Rangifer tarandus platyrhynchus). Parasitology **120**, 297–311 (2000). https://doi.org/10.1017/S0031182099005430
70. M.E. Taghavizadeh Yazdi, M. Darroudi, M.S. Amiri, H. Zarrinfar, H.A. Hosseini, M. Mashreghi, H. Mozafarri, A. Ghorbani, S.H. Mousavi, Antimycobacterial, anticancer, antioxidant and photocatalytic activity of biosynthesized silver nanoparticles using berberis integerrima. Iranian Journal of Science and Technology, Transactions A: Science **46**(1), 1–11 (2022). https://doi.org/10.1007/s40995-021-01226-w